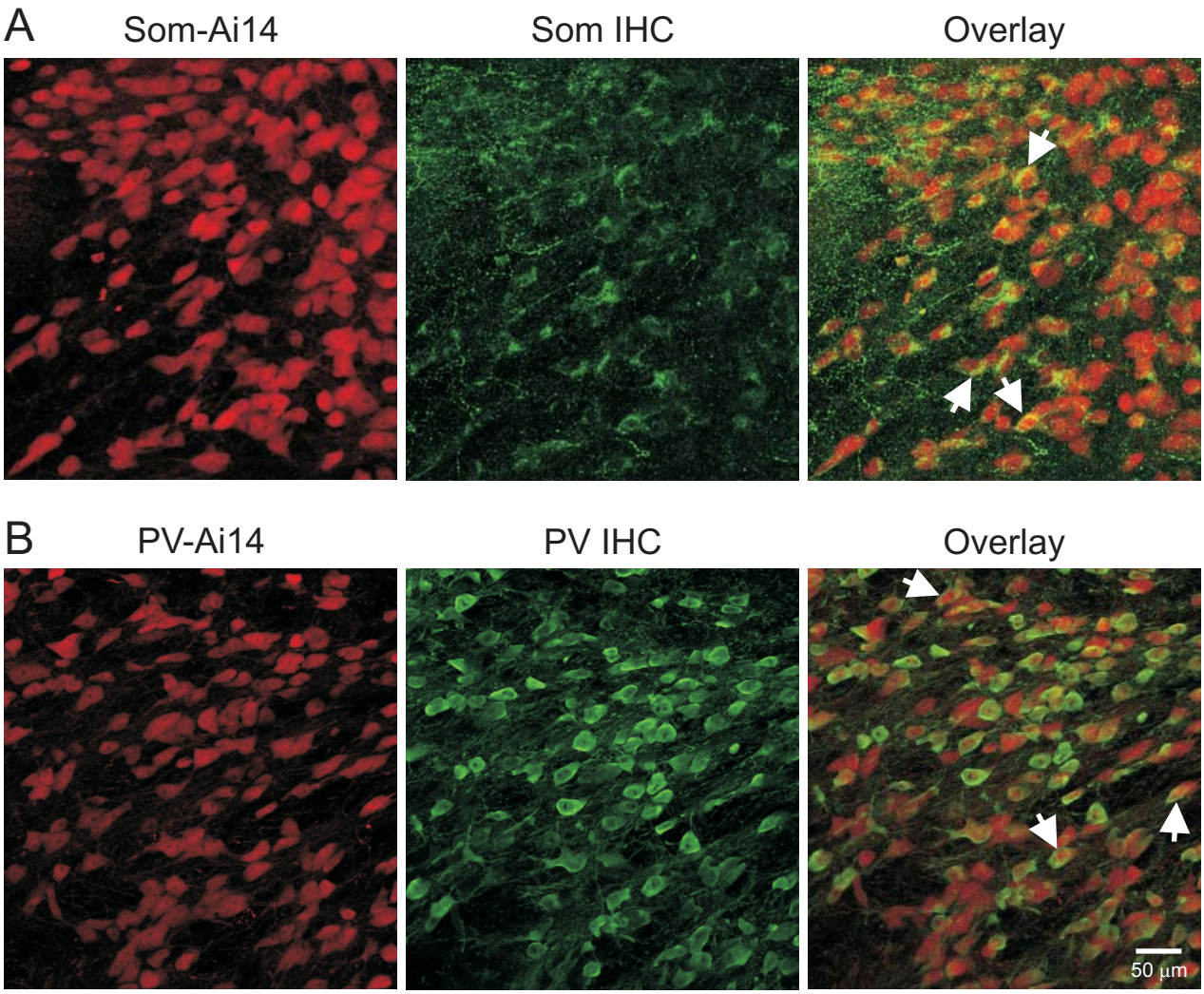

Supplemental Figure S1. TdTomato from SOM and PV-Cre x Ai14 animals colocalizes with somatostatin and parvalbumin in the nRT (related to Figure 1). A. Brain slice from a SOM-Cre x Ai14 animal (left). Image of somatostatin stain in green (middle). Image overlaying red and green showing co-labeling of red and green (arrowheads). Scale bar, 50 µm. For the SOM-Cre animals, the percentage of Cre-targeted neurons that showed SOM immunofluorescence (specificity) was 90±1%, and the percentage of SOM-immunolabeled cells that were positive for Cre (efficiency) was 98±1%. **B.** Brain slice from a PV-Cre x Ai14 animal (left). Image of parvalbumin stain in green (middle). Image overlaying red and green showing co-labeling of red and green (arrowheads). Scale bar, 50 µm. For the PV-Cre animals, the percentage of Cre-targeted neurons that showed PV immunofluorescence was 92± 3% and the percentage of PV-labeled cells that were positive for Cre was 97±1%.

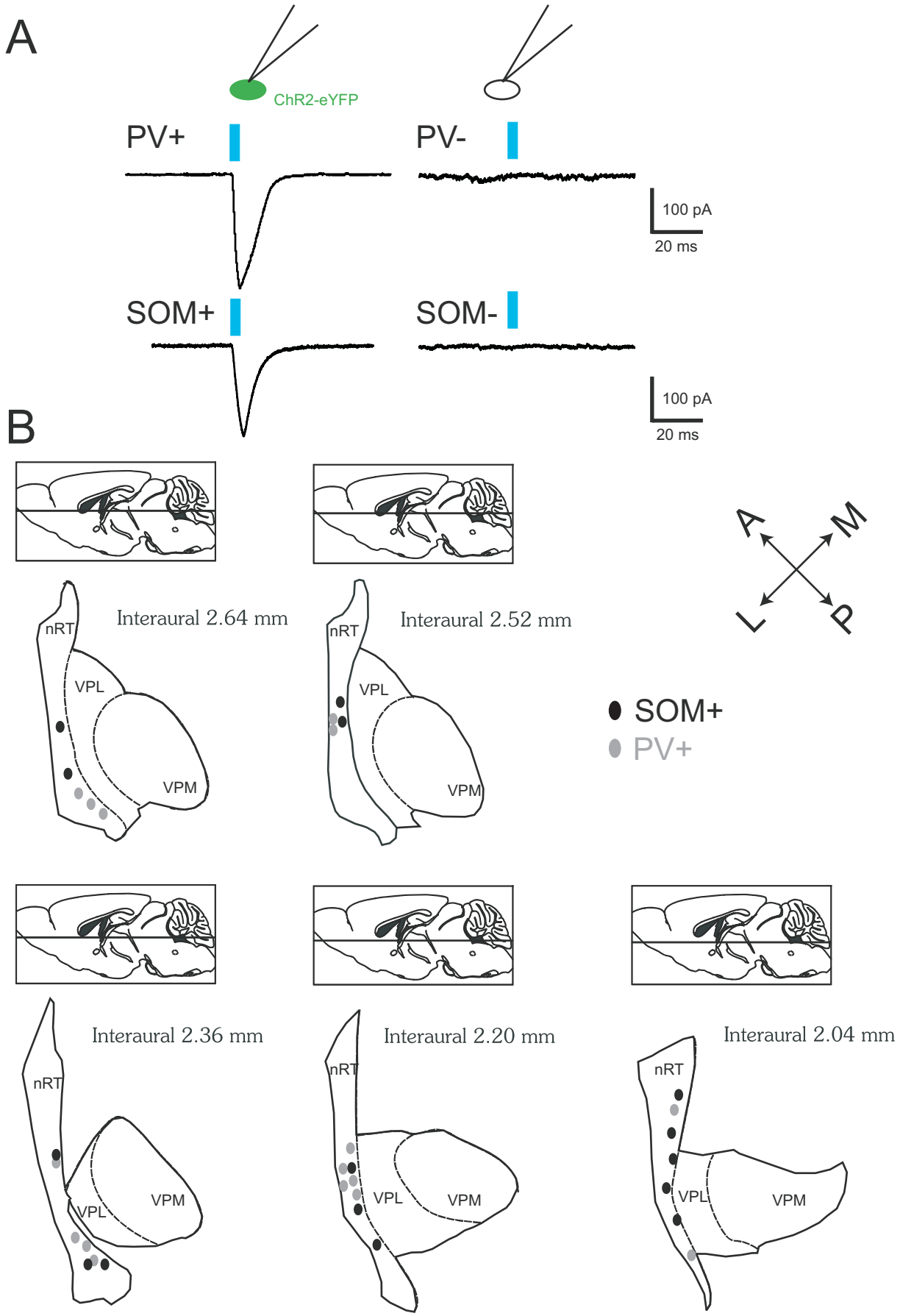

Supplemental Figure S2. Identification of Recorded PV and SOM Neurons in nRT (related to Figure 2). A. PV or SOM cells were identified according to their activation with blue light (450 nm, see direct ChR2 current evoked with blue light in "+" but not "-" cells) in thalamic slices from PV-Cre x Ai32 and SOM-Cre x Ai32 mice, respectively. **B.** Summary diagram showing the location of recorded cells in the SOM-Cre x Ai32 and PV-Cre x Ai32 animals used for intrinsic property analysis.

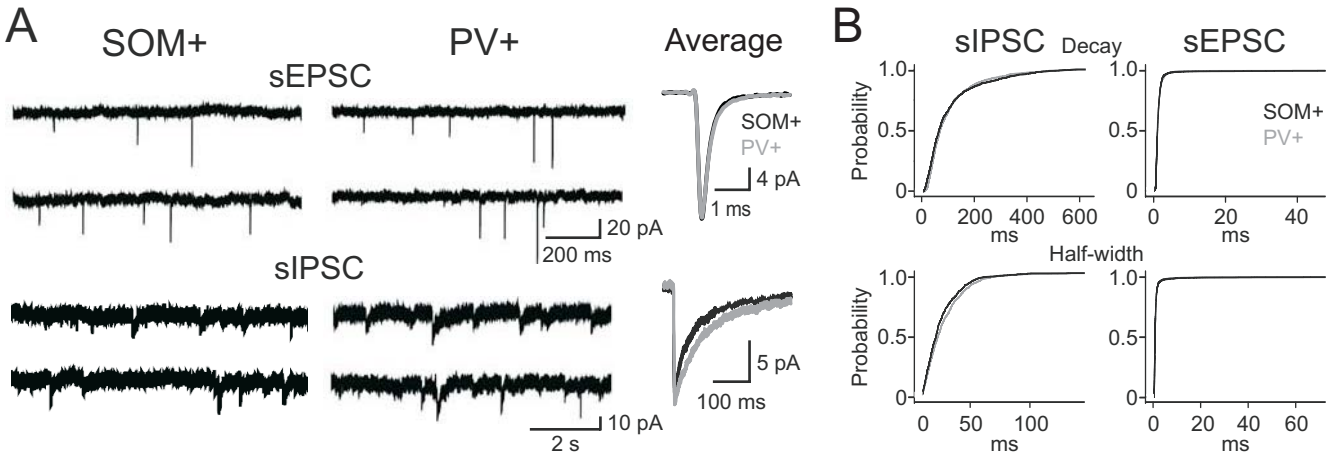

Supplemental Figure S3. Spontaneous Excitatory and Inhibitory Synaptic Currents in PV and SOM Cells (related to Figure 2). A. *Left:* Representative traces of spontaneous excitatory postsynaptic currents (sEPSC) (top) and spontaneous inhibitory postsynaptic currents (sIPSC) (bottom) in SOM (left) and PV cells (right). *Right:* Representative average sEPSC (top) and sIPSC (bottom) traces taken from single cell recordings. **B-C.** Cumulative probability distributions for decay tau (B) and half-width (C) of sEPSCs (right) and sIPSCs (left). Cumulative probability distributions and KS-test p-values were generated using the bootstrap method with 1000 iterations from 17 PV and 10 SOM cells using 80 events/cell for sEPSCs per iteration (three mice for each group) and 30 events/cell for sIPSCs from 12 PV and 8 SOM cells (three mice for SOM group and five mice for PV group). The probability distributions were similar between SOM and PV neurons ($p>0.1$ for all the parameters).

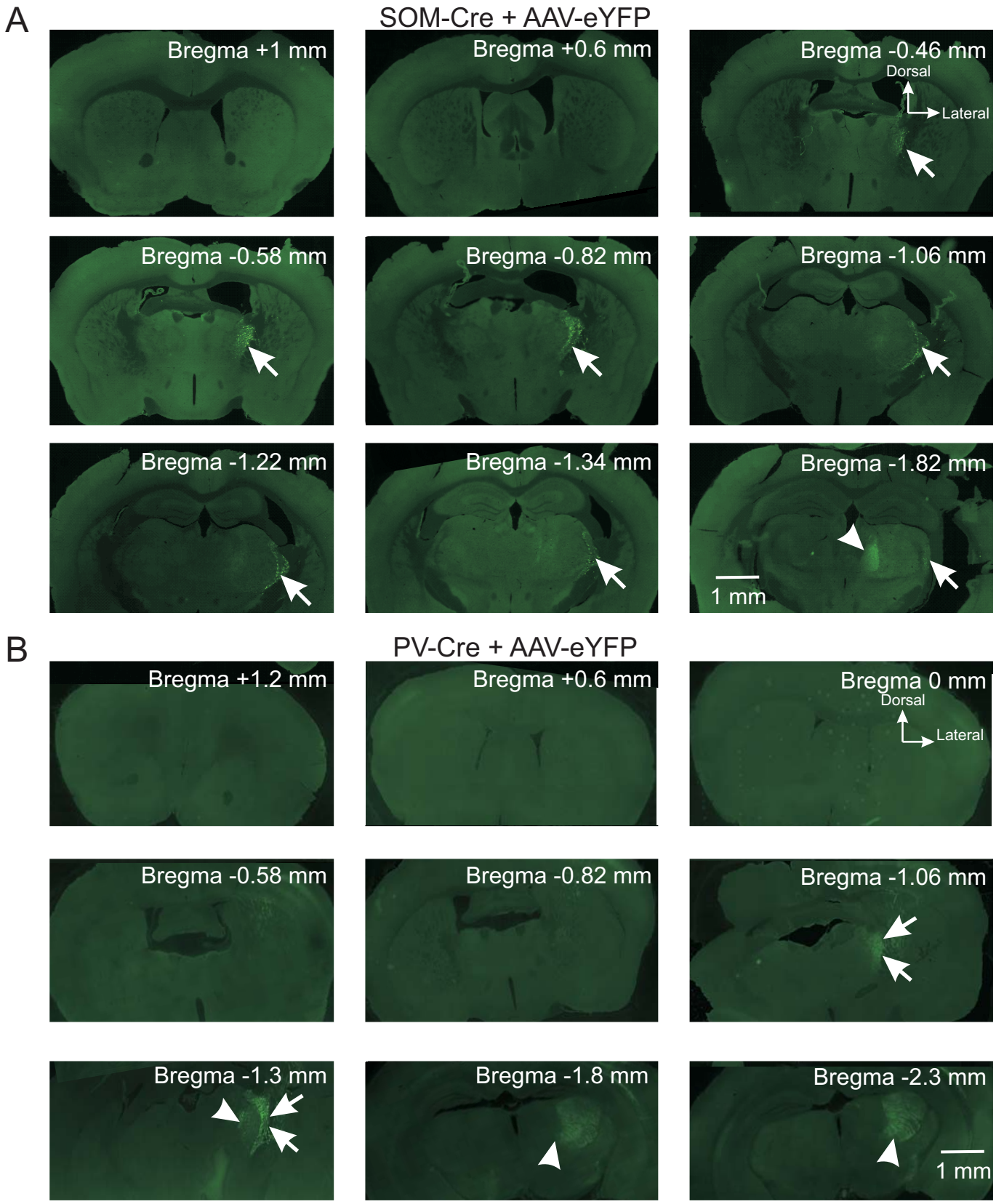

Supplemental Figure S4: nRT Stereotaxic Injection of AAV-DIO-ChR2-eYFP in SOM- and PV-Cre Mice Results in Specific Expression of eYFP in nRT Cells (arrows) and Axons (arrowheads) (related to Figure 3).

A. Images of coronal brain sections taken from a SOM-Cre mouse that received two 200 nl nRT stereotaxic injections of AAV-DIO-ChR2-eYFP (see Experimental Procedures for injection coordinates); mouse brain was perfused 4 weeks after viral injection in nRT. B. Images of coronal brain sections taken from a PV-Cre mouse that received two 200 nl nRT stereotaxic injection of AAV-DIO-ChR2-eYFP; mouse brain was perfused 4 weeks after viral injection in nRT. Viruses were only injected in middle sections of the nRT (1.3 mm posterior to Bregma). Arrows indicate eYFP+ cell bodies, arrowheads indicate eYFP+ fibers. The depicted results were found in 4 PV-Cre and 4 SOM-Cre mice. In all mice, SOM eYFP+ fibers were observed mainly in intralaminar nuclei whereas the PV eYFP+ fibers were observed mainly in VB and Po.

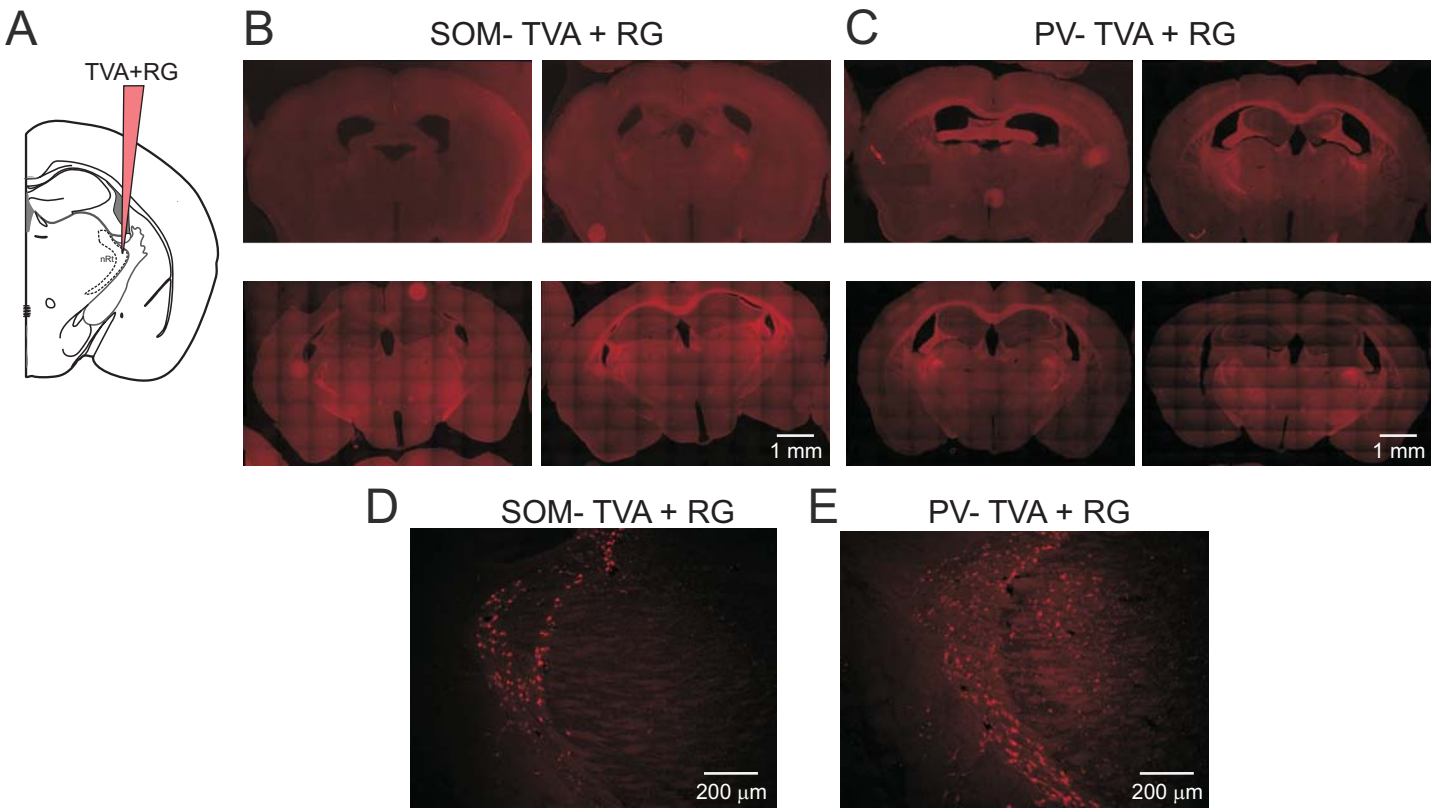

Supplemental Figure S5. nRT Stereotaxic Injection of TVA-mCherry + RG viruses in SOM and PV Cre Mice Results in Specific Expression in nRT Cells and Axons (related to Figure 6).
A. Experimental design: SOM-Cre or PV-Cre mice were injected in the middle nRT (1.3 mm posterior to Bregma, see Experimental Procedures for details) with AAV expressing TVA-mCherry and rabies glycoprotein (RG) in a Cre-dependent manner. **B.** Representative images of coronal brain sections taken from a SOM-Cre mouse that received two 100 nl nRT stereotaxic injections of viral constructs containing TVA-Cherry + RG; mouse brains perfused 21 days after viral injection in nRT. **C.** Representative images of coronal brain sections taken from a PV-Cre mouse that received double 100 nl nRT stereotaxic injection of viral constructs containing TVA-Cherry + RG; mouse brains perfused 4–6 weeks after viral injection in nRT. **D.** Higher magnification image from the SOM-Cre mouse shows mCherry expression in nRT. **E.** Higher magnification image from the PV-Cre mosue shows mCherry expression in nRT and a minor expression in VPM. Notably, the minor staining in VPM did not affect the results depicted in Figure 6, given that in all mice the same major input region was found to be S1 Barrel cortex and VPM which are known to project onto nRT from numerous previous studies (see text for details). The viral constructs were only injected in middle sections of the nRT (1.3 mm posterior to Bregma).

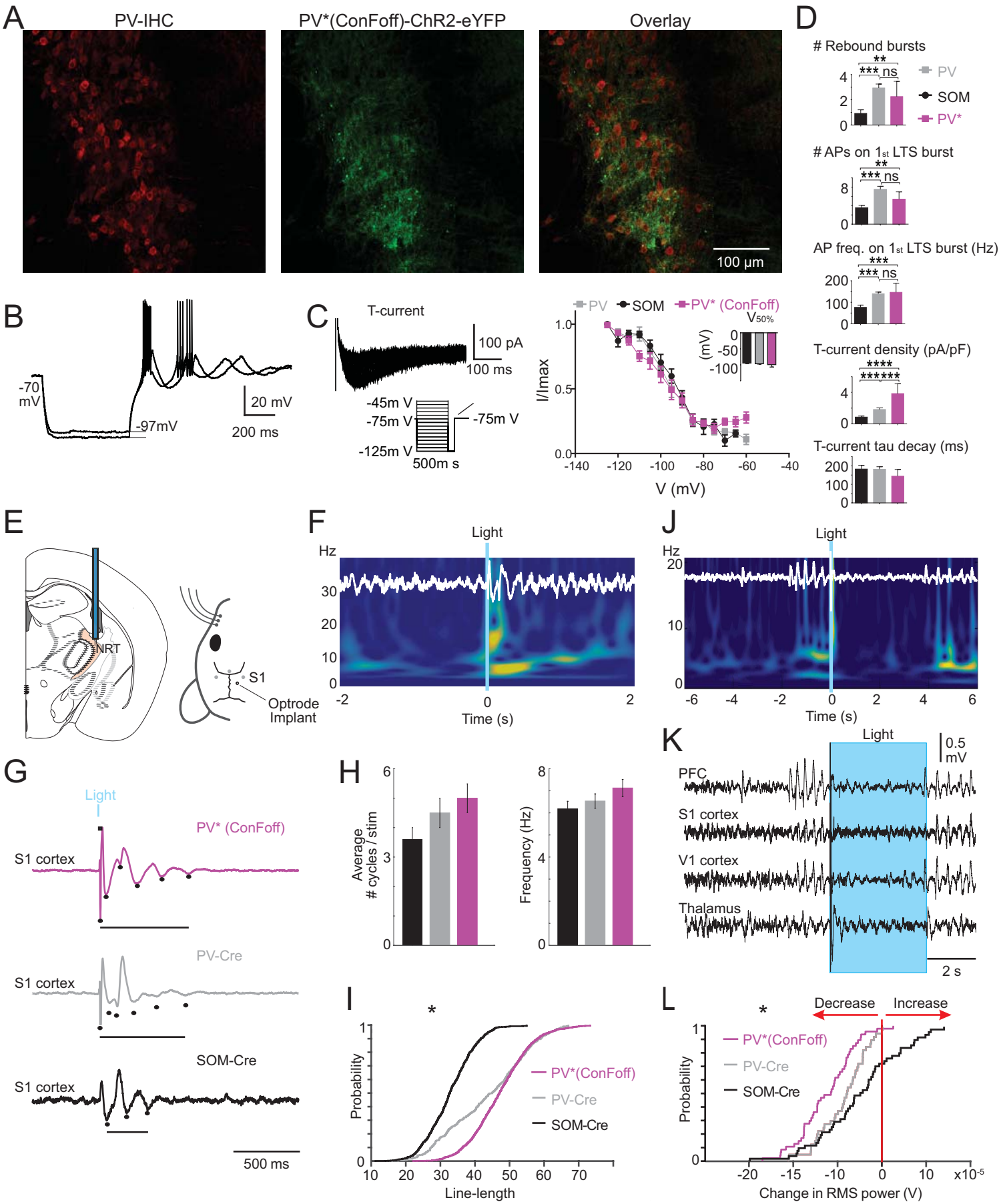
A
PV-IHC
PV*(ConFoff)-ChR2-eYFP
Overlay
100 µm
B
-70 mV
-97mV
20 mV
200 ms
C
T-current
100 pA
100 ms
-45m V
-75m V
-125m V
-75m V
500m s
PV
SOM
PV* (ConFoff)
V50%
I/Imax
V (mV)
D
Rebound bursts
APs on 1st LTS burst
AP freq. on 1st LTS burst (Hz)
T-current density (pA/pF)
T-current tau decay (ms)
PV
SOM
PV*
E
NRT
S1
Optrode Implant
F
Light
Hz
Time (s)
J
Light
Hz
Time (s)
G
Light
PV* (ConFoff)
S1 cortex
PV-Cre
S1 cortex
SOM-Cre
S1 cortex
500 ms
H
Average # cycles / stim
Frequency (Hz)
K
Light
0.5 mV
PFC
S1 cortex
V1 cortex
Thalamus
2 s
I
Probability
PV*(ConFoff)
PV-Cre
SOM-Cre
Line-length
L
Decrease
Increase
Probability
PV*(ConFoff)
PV-Cre
SOM-Cre
Change in RMS power (V)

Figure S6

Supplemental Figure S6. Validation of INTRSECT approach (related to Figure 7). **A.** Brain slice from a Cre/Flp animal that received two 200 nl nRT stereotaxic injections of CreON/FlpOFF-ChR2-eYFP (middle) and has been stained for parvalbumin in red (left). Image overlaying red and green showing co-labeling of red and green image of somatostatin stain in green (middle). Scale bar, 25 μm. **B**. Representative traces showing that PV* cells expressing ChR2, exhibit strong post-inhibitory rebound burst firing upon hyperpolarization, induced by -120 and -80 pA current pulses. **C**. *Left*, Representative traces showing T-type calcium current obtained with the SSI protocol for PV* cells of the nRT, *Right*, Normalized current amplitude plotted as a function of the pre-pulse membrane potential that is best-fitted with a Boltzmann function (R2=0.99 for both fits). *Inset*, Half-maximal voltage (V50%) taken from Boltzmann function (data from 11 PV cells from 4 mice, 10 SOM cells from 8 mice and 9 PV* cells taken from 3 mice). **D.** Comparison of intrinsic properties between PV-Cre, SOM-Cre, and PV* mice: number of rebound bursts, number of action potentials on first rebound burst, frequency of action potentials on first rebound burst, t-type current density, t-current decay time constant. All data in D are represented as mean ± SEM, compared using a Mann-Whitney test, with α=0.05. (*p<0.05, **p<0.01, ***p<0.001). Notably, the resting membrane potential was similar in PV and PV* cells (PV: -70.2 ± 2.7 mV, n= 12 cells from 4 mice; PV*: -73.4 ± 2.1 mV, n=10 cells from 3 mice; p=0.4; Mann Whitney test). The action potential properties were similar in PV and PV* cells including threshold (PV: -50.3 ± 0.9 mV, n= 12 cells from 4 mice; PV*: -52.4 ± 1.7 mV, n=10 cells from 3 mice; p=0..3, Mann Whitney test) and duration (PV: 1.4 ± 0.1 ms, n=12 cells from 4 mice; PV*: 1.4 ± 0.1, n=10 cells from 3 mice; p=0.9; Mann Whitney test). The quantification was not included in the figure for clarity. **E.** Diagram of recording and stimulation locations for *in vivo* experiments. *Left*: Approximate location of an optrode (i.e., optical fiber and two tungsten depth electrodes implanted unilaterally in the nRT. *Right:* Optrode and ECoG recording sites (S1 – somatosensory cortex) and optrode on mouse skull. **F.** Representative wavelet time-frequency spectrograms and associated single-trial ECoG traces from ipsilateral S1 in PV* mice. Blue rectangles indicate stimulation of ChR2-expressing PV* neurons (unilateral, single, 20 ms-long light pulse, 450 nm). **G.** Representative ECoG traces averaged per mouse (n=100–300 sweeps/trial) in PV* (purple), PV-Cre (grey), and SOM-Cre (black) mice. Blue line, stimulation of ChR2-expressing neurons (unilateral, single, 20 ms-long light pulse, 450 nm); black line, duration of the oscillatory response in the ECoG. **H.** Mean ± SEM of cycle number and frequency (Hz) per evoked oscillation in S1 cortex (averages from 1400 trials per n=6 ConFoff mice, 400 trials per n=2 PV-Cre mice, 1000 trials per n=5 Som-Cre mice). **I.** Cumulative probability distribution of the line-length of the 7–15 Hz frequency in S1 ECoG, evoked by stimulation of nRT (PV* vs. PV vs. SOM stimulation. ***p<.001, two-sample KS test). **J.** Representative wavelet time-frequency spectrogram and associated single-trial ECoG traces showing optical stimulation during an ongoing spike-and-wave seizure recorded from PV* mice. **K.** Corresponding and additional ECoG traces from the wavelet shown in J. ECoG traces from PFC, ipsilateral S1 cortex, and ipsilateral V1 cortex are shown, with LFP and MU from nRT. Blue box denotes duration of light stimulation. **L.** Population cumulative probability distribution plots of change in RMS power (post-pre) from PV* (n = 6, purple), PV-Cre (n = 4, grey) and SOM-Cre (n = 5, black) mice for all seizure interruption trials comparing RMS power 2 s before and 2 s after the stimulation (PV vs. SOM, PV vs. PV*. *p<.05. PV* vs SOM, ***p<.001).

SUPPLEMENTAL TABLES

Table S1: Passive and active electric membrane properties of PV and SOM neurons in nRT										
	Cm (pF)	**Vm (mV)**	**Rin (MΩ)**	**τ_m (ms)**	**AP threshold (mV)**	**AP duration (ms)**	**Rheobase (pA)**	**F-I Slope (Hz/pA)**	**# Cells**	**# Mice**
PV	64.1 ±6.12	-70.2 ± 2.7	496.3 ± 55.7	46.6 ± 4.4	-50.3 ± 0.9	1.44 ± 0.09	46.7 ± 8.6	0.38 ± 0.05	12	4
SOM	59.3 ± 5.5	-71.4 ± 3.0	494.8 ± 64.2	38.1 ± 3.8	-51.4 ± 1.1	1.54 ± 0.09	67.1 ± 9.0	0.4 ± 0.04	18	8
p-value	ns	ns	ns	ns	ns	ns	ns	ns		

Table S1: Passive and active electric membrane properties of PV and SOM neurons in nRT, related to Figure 2. Data represented as mean±SEM, compared using a Mann-Whitney test, with α=0.05. ns, non significant, p>0.05.

Table S2. Properties of spontaneous excitatory and inhibitory postsynaptic currents in PV and SOM neurons in nRT									
		Rise time (ms)	**τ_{Decay} (ms)**	**Half-width (ms)**	**Amplitude (pA)**	**Charge (fC)**	**Interval (s)**	**# Cells**	**# Mice**
sIPSC	**PV**	1.5 ± 0.1	92.4 ± 13.5	28.8 ± 1.3	14.1 ± 0.5	234 ± 13.5	2.7 ± 0.5	12	5
	SOM	1.5 ± 0.1	90.6 ± 28.8	26.5 ± 0.8	15.8 ± 1.6	219 ± 17.6	2.7 ± 0.9	8	3
	p-value	0.53	0.95	0.45	0.71	0.8	0.64		
sEPSC	**PV**	0.3 ± 0.01	16.6 ± 1.0	1.2 ± 0.1	22.3 ± 1.4	28.6 ± 1.95	0.4 ± 0.1	15	3
	SOM	0.3 ± 0.01	13.9 ± 1.6	1.3 ± 0.2	19.7 ± 1.2	25.9 ± 1.78	0.5 ± 0.1	10	3
	p-value	ns	ns	ns	ns	ns	ns		

Table S2: Properties of spontaneous excitatory and inhibitory postsynaptic currents in PV and SOM cells, related to Figure 2. Interval indicates the average inter-event duration. Data represented as mean±SEM, compared using a Mann-Whitney test, with α=0.05. ns, non significant, p>0.05.

EXPERIMENTAL PROCEDURES

Experimental Model Details

We performed all experiments per protocols approved by the Institutional Animal Care and Use Committee at the University of California, San Francisco and Gladstone Institutes. Precautions were taken to minimize stress and the number of animals used in each set of experiments. Animals were separately housed after surgical implants.

Somatostatin (SOM)-Cre mice (SOM-IRES-Cre, IMSR_JAX:013044; mixed C57BL/6;129S4), Parvalbumin (PV)-Cre mice (PV-Cre, IMSR_JAX: 017320; C57BL/6 congenic), Rosa26-tdTomato reporter mice (Ai14, IMSR_JAX:007914; congenic C57BL/6 generously provided by Dr. Ken Nakamura, Gladstone Institutes); Rosa26-ChR2(H134R)-EYFP reporter mice (Ai32, IMSR_JAX:012569; mixed C57BL/6;129S4), C57BL/6J mice (wild-type, IMSR_JAX:000664), and PV-Cre/SOM-Flp mice (PV-p2A-Cre, SOM-IRES-Flp (Fenno et al., 2014).), were housed in the Research Animal Facility at the Gladstone Institutes. Both male and female mice were used for these experiments.

METHOD DETAILS

Viral injections

Stereotaxic viral injections were carried out as described (Paz et al., 2011, 2013).

For eYFP tracing studies (Figure 3) (UNC Joint Vector Laboratories, SCR_002448), a total of 200-500 nl of concentrated virus (2×10^{12} genome copies per milliliter) carrying genes for eYFP alone (rAAV5/EF1a-EYFP for PV-Cre or SOM-Cre) were injected in nRT. Different injections volumes were found to have comparable projection patterns. Images shown are for mice containing a total of 500 nl.

For optogenetic experiments, both *in vivo* (Figure 7) and *in vitro* (Figure 3) a total of 400 nl of concentrated virus (2×10^{12} genome copies per milliliter) carrying genes for ChR2 (rAAV5/EF1a-ChR2-EYFP for PV-Cre or SOM-Cre mice; rAAV5/hSyn-Con/Foff-hChR(H134R)-eYFP (INTRSECT virus) for PV-Cre/SOM-Flp mice) was used.

The virus was injected stereotaxically unilaterally into the right nRT of P30-P60 mice. For the PV-Cre, SOM-Cre mice, and PV-Cre/SOM-Flp mice, the stereotaxic coordinates of the injections were 1.3–1.6 mm posterior to Bregma, 2.0–2.1 mm lateral to the midline. Two injections, each containing half the total volume (100-250 nl), were made at 2.6 and 3.0 mm ventral to the cortical surface. We allowed the viruses to express for anywhere between 3 weeks and 3 months, depending on the nature of the experiment.

For trans-synaptic labeling (Figure 6), 200-400 nl (two 100 nl or 200 nl injections) of a 1:1 mixture of AAV CAG-FLEx-RG and AAV CAG-FLEx-TVA-mCherry were first injected using the same coordinates to target nRT as above, followed by a second injection 2 weeks later of 200 nl (two 100 nl injections) of pseudotyped RV (ΔG-GFP+EnvA). To avoid viral spreading into neighboring areas, we used a smaller amount of virus for trans-synaptic labeling than we did for optogenetic and anterograde tracing experiments. Animals were kept alive for 7 days after RV injection to allow trans-synaptic spreading and sufficient GFP labeling in presynaptic cells. No additional labeling was required to observe GFP or mCherry signal.

Immunostaining, Microscopy, and Image Analysis

Mice were anesthetized with a lethal dose of ketamine (300 mg/kg) and xylazine (30 mg/kg) and perfused with 4% paraformaldehyde in 1X PBS. Serial coronal sections (50 μm thick) were cut on a Leica SM2000R Sliding Microtome. Sections were incubated with antibodies directed against PV (1:2000, mouse, Sigma, P3088, AB_47732) or SOM (1:1000, mouse, Peninsula Labs, AB_2302603) overnight at 4°C. After wash, sections were incubated with Alexa Fluor–conjugated secondary antibodies (1:300, Thermo Fisher Scientific, A-11029) for 2 h at room temperature. Sections were mounted in an antifade medium (Vectashield). To measure the proportion of PV+SOM-, PV-SOM+, and PV+SOM+ cells, we used immunostaining for PV as a corollary for PV expression and the tdTomato reporter as a corollary for SOM expression on sections obtained from the SOM-Ai14 mice.

For the analysis shown in Figure 1, confocal imaging was performed using a confocal laser scanning microscope (LSM880, Zeiss) equipped with a Plan Apochromat 20x/"0.75" NA or 63x/1.4 NA oil immersion objective lens. A multi-line Argon laser was used for 488 nm excitation of the AlexaFluor488 and a 561 nm HeNe laser for excitation of tdTomato. Slices used for imaging corresponded to a Bregma location of approximately -1.3 posterior from Bregma, ± 0.2 mm. A series of 20x images were taken of the head, middle, and tail sections of nRT from 2 slices per mouse (n=4 mice) using a Z-stack to capture the entirety of the labeled cell population within the focal plane. These images were used for cell counting. Cells were counted as either green only (PV+), red only (SOM+) or both green and red (PV+ SOM+, referred to as "coexpressing" in Figure 1) using Bitplane Imaris (SCR_007370). The nRT was outlined using the PV signal and confirmed using the mouse brain atlas (Franklin and Paxinos, 2007). A separate set of 63x images using a Z-stack were also taken to more clearly show non-overlapping populations. Bitplane Imaris (SCR_007370) was used to render a 3D image of each region from nRT. For the 63x

image, processing and figure preparations were performed using a combination of Bitplane Imaris (3D rendering of Z-stacks) and Fiji (http://fiji.sc/wiki/index.php/Fiji). For Figure 6, images were taken with a Biorevo BZ-9000 Keyence microscope at 20x-40x. Input cells were quantified by measuring the total number of green cells in the observed brain nuclei. Ratios were taken by dividing input cells per nuclei over total cells counted.

Immunostaining of Human Tissue

Control human thalamic tissues (n=3) were obtained from two males (55- and 77-years-old) and one female (77-years-old) subjects who died from causes not linked to brain diseases. None of them had a history of neurological disorders. The three subjects were processed for autopsy in Saint Borbála Hospital, Tatabánya, Department of Pathology. Informed consent was obtained for the use of brain tissue and for access to medical records for research purposes. Tissue was obtained and used in a manner compliant with the Declaration of Helsinki. All procedures were approved by the Regional and Institutional Committee of Science and Research Ethics of Scientific Council of Health (ETT TUKEB 31443/2011/EKU (518/PI/11)). Brains were removed 4–5 h after death. The internal carotid and the vertebral arteries were cannulated, and the brains were perfused first with physiological saline (using a volume of 1.5 L in 30 min) containing heparin (5 ml), followed by a fixative solution containing 4% paraformaldehyde, 0.05% glutaraldehyde and 0.2% picric acid (vol/vol) in 0.1 M PB, pH 7.4 (4–5 l in 1.5–2 h). The thalamus was removed from the brains after perfusion, and was postfixed overnight in the same fixative solution, except for glutaraldehyde, which was excluded.

Postmortem formalin fixed human thalami were cut on a vibratome with section thickness of 50 µm. The sections were incubated with 10% normal goat serum followed by the overnight incubation with the mixture of rabbit anti-parvalbumin (1:2000; Swant, Marly, Switzerland, code PV25, AB_10000344) and rat anti-somatostatin (1:500; Merck Millipore, code MAB 354, AB_2255365). Parvalbumin was visualized with the fluorescent dye Alexa488 conjugated goat anti-rabbit (1:500; Molecular Probes, Leiden, The Netherlands, code A-11001). Whereas somatostatin with biotinylated-SP (long spacer) goat anti-rat (1:300; Jackson Immuno Research, Newmarket, Suffolk, UK, code 112-065-167) and by avidin-biotinylated horseradish peroxidase complex (1:300; ABC, Vector, code PK-6200). This immunoreaction was visualized using nickel intensified DAB (DAB-Ni) as the chromogen.

Slice preparation

Mice were euthanized with 4% isoflurane, perfused with ice-cold sucrose cutting solution containing 234 mM sucrose, 2.5 mM KCl, 1.25 mM NaH_2PO_4, 10 mM $MgSO_4$, 0.5 mM CaCl2, 26 mM $NaHCO_3$, and 11 mM glucose, equilibrated with 95% O_2 and 5% CO_2, pH 7.4, and decapitated. We prepared 250 µm-thick horizontal thalamic slices containing VB thalamus and nRT with a Leica VT1200 microtome (Leica Microsystems). We incubated the slices, initially at 32 °C for 1 h and then at 24–26 °C, in artificial cerebro-spinal fluid (ACSF) containing 126 mM NaCl, 2.5 mM KCl, 1.25 mM NaH_2PO_4, 2 mM $MgCl_2$, 2 mM $CaCl_2$, 26 mM $NaHCO_3$, and 10 mM glucose, equilibrated with 95% O_2 and 5% CO_2, pH 7.4. The thalamic slice preparation was performed as described (Paz et al., 2011, 2013).

Patch-clamp electrophysiology from thalamic slices

Recordings were performed as previously described (Paz et al., 2011, 2013). We visually identified nRT and thalamocortical neurons by differential contrast optics with a Zeiss (Oberkochen) Axioskop microscope and an infrared video camera. Recording electrodes made of borosilicate glass had a resistance of 2.5–4 MΩ when filled with intracellular solution. Access resistance was monitored in all the recordings, and cells were included for analysis only if the access resistance was <25 MΩ. Cells were filled with 0.2–0.5% biocytin (Sigma-Aldrich), and whole slices were fixed and processed using standard avidin–biotin peroxidase (Horikawa and Armstrong, 1988). We corrected the potentials for -15 mV liquid junction potential. Intrinsic and bursting properties and spontaneous and evoked inhibitory post-synaptic currents (IPSCs) were recorded in the presence of kynurenic acid (2 mM, Sigma). For IPSCs, the internal solution contained 135 mM CsCl, 10 mM HEPES, 10 mM EGTA, 5 mM QX-314 (lidocaine N-ethyl bromide), and 2 $MgCl_2$, pH adjusted to 7.3 with CsOH (290 mOsm). Excitatory post-synaptic currents (EPSCs) were recorded in the presence of picrotoxin (50 µM, Tocris). For EPSCs and current-clamp recordings, the internal solution contained 120 mM potassium gluconate, 11 mM KCl, 1 mM $MgCl_2$, 1 mM $CaCl_2$, 10 mM HEPES, and 1 mM EGTA, pH adjusted to 7.4 with KOH (290 mOsm). Immunofluorescence was assessed with a Biorevo BZ-9000 Keyence microscope.

Extracellular thalamic oscillations
Horizontal slices (400 μm) containing the VB and nRT were placed in a humidified, oxygenated interface chamber and perfused at a rate of 2 mL/min at 34°C with oxygenated ACSF prepared as described above and supplemented with 300 μM glutamine for cellular metabolic support. Extracellular MU recordings were obtained with a 16-channel multi-electrode array (Neuronexus) placed in the nRT and VB. Signals were amplified at 10,000x and band-pass filtered between 100 Hz and 6 kHz using the RZ5 from Tucker-Davis Technologies (TDT, SCR_006495). PV and SOM neurons of the nRT were locally activated by a 450 nm blue light optical pulse (0.8–5 mW, 100 ms duration every 10 s) delivered to the nRT via a 200 μm optical fiber (Thorlabs). Sweeps were repeated 10–30 times in a single recording. Position of recording probe was visually checked for each recording to confirm position of electrodes in nRT and VB.

***In vivo* data acquisition during free behavior**
We designed devices containing multiple screws for acquisition of electrocorticogram (ECoG) signal, along with local field potential (LFP) and multi-unit (MU) signal recoded from tungsten electrode wires that were positioned approximately 300 μm from the tip of an optic fiber (200 μm core, ThorLabs) (Paz et al., 2013). Cortical screws were implanted in S1 (-0.5 mm posterior from Bregma, ± 3.25 mm lateral), in V1 (-2.9 mm posterior from Bregma, ± 3.25 mm lateral), or in lieu of two V1 channels, in PFC (0.5 mm anterior to Bregma, 0 mm lateral). For manipulation of nRT, optrodes were implanted at -1.3 mm posterior from Bregma, 2.1 mm lateral, and 2.5 mm deep. Mice were allowed to recover for at least one week before recording. ECoG signals were recorded using RZ5 (TDT) and sampled at 1221 Hz, and thalamic extracellular MU signals were sampled at 24 kHz. A video camera that was synchronized to the signal acquisition was used to continuously monitor the animals. Each recording trial lasted 30–60 min. To control for circadian rhythms, we housed our animals using a regular light/dark cycle, and performed recordings between roughly 11:00 AM and 4:00 PM.

***In vivo* optogenetics**
We simultaneously passed a fiber optic with an inline rotating joint (Doric) through a concentric channel in the electrical commutator, and connected it to the 200 μm core fiber optic in each animal's headpiece while recording ECoG/MU. The fiber optic was connected to a 450 nm wavelength laser control box, which was triggered externally using the RZ5 (TDT). The tip of the fiber rested 300 μm from the most dorsal tungsten electrode on each optrode to allow maximal activation of the nRT without physically obstructing the electrodes. We used 8–20 mW of 450 nm blue light, measured at the end of the optical fiber before connecting to the animals. nRT cells were stimulated using 20 ms light pulses, delivered every 10 seconds.

Optogenetic disruption of Seizures
We used a low dose of the proconvulsant pentylenetetrazol (PTZ, 35 – 60 mg/kg) injected intraperitoneally to induce pharmacological seizures in mice who were previously instrumented for simultaneous ECoG recordings and thalamic optical stimulation as described above. After injection, mice were placed in their home cage and left to behave freely. Experimenters visually monitored ECoG and thalamic LFP/MUA signal for spike-and-wave seizures and brief generalized spiking seizure episodes (< 10 s). During seizures that were > 1 s in length, experimenters manually triggered the optical stimulation (4 s, 450 nm, 25 – 35 mW measured at the end of the optical fiber before connecting to the animals). Trials were considered to be valid if the experimenter triggered the light during an ongoing seizure. A custom Matlab script was used to identify valid stimulation trials off-line after data collection. The number of trials per mouse ranged from 3 - 23, with the majority of mice having at least 5 trials sampled per mouse.

Optogenetic manipulation of Somatosensory Behavior
To assess somatosensory-related behaviors, we used the same mice who were instrumented for optical stimulation experiments in a modification of the adhesive removal task behavior involving the front paws and whisker pad (Bouet et al., 2009). Briefly, on the test day, we restrained the mice and applied a piece of zinc oxide tape (5 mm x 10 mm) to the left whisker pad area as shown in Figure 7M. Mice were immediately returned to their home cage, and we recorded the contact time (time to touch the tape), removal time (time to remove tape) and grooming time (time spent grooming facial area after tape was removed) per trial. Each mouse was subjected to three trials spread over ~20 minute per condition. Mice were handled for 1-2 days to habituate to the experimenter, and then subjected to a baseline test day to reduce novelty associated with the task. We then performed successive test days of sham (no optical stimulation), light stimulation (10 s light stimulation upon attachment of tape to the whisker pad), sham (no optical stimulation) and a light alone trial (no tape used). Light stimulation used 450 nm of blue light, 15 mW

measured at the end of the optical fiber before connecting to the animals. An experimenter measured time spent grooming off-line using video scoring. Responses across trials were averaged per condition. Trials were excluded if the tape fell off prior to the mouse being returned to their home cage.

QUANTIFICATION AND STATISTICAL ANALYSIS

All numerical values are given as means and error bars are Standard Error of the Mean (SEM) unless stated otherwise. Parametric and non-parametric tests were chosen as appropriate. Data analysis was performed with MATLAB (SCR_001622), Origin 9.0 (Microcal Software, SCR_002815), GraphPad Prism 6 (SCR_002798), R-project, and SigmaPlot (SCR_003210).

Image analysis and cell quantification

For cell quantification, a single image of either the head, middle, or tail of nRT was analyzed for labeled cell counts (Fig. 1E). A combination of automated cell-counting algorithms was applied using the "shape" feature of Imaris to count all labeled somas in either the red or the green channel. To determine the fraction of cells that were double-labeled, an additional mean intensity filter for the green channel was applied to the red channel to identify populations that were double-labeled. Note, PV labeling that was clearly perisomatic was used to identify cells that were double-labeled. The remaining PV label that was punctate that presumably corresponded to fibers and other unidentified cellular compartments was not considered to be cellular labeling because the origin of the labeling was not clear. Final cell counts were expressed as a relative proportion of each group, with the total cell counts corresponding to counts from the "red" plus "green condition data are represented as mean and error bars are standard error of the mean. Data were analyzed using Mann-Whitney test, with alpha = 0.05 (*p<0.05, **p<0.01, ***p<0.001, ****p<0.0001). For Figure 1E, a total of 4 mice were used for analysis (n = 2 slices per mouse, 1 image per nRT region).

Comparison of electrophysiological properties between PV and SOM nRT cells

For recordings of 14 PV cells and 16 SOM cells, spikes over -20 mV during 0.6 sec stimulations of 20 to 400 pA were counted automatically using custom R-Project code. Spiking frequency was computed as the spike count divided by the stimulus duration (Fig. 2E). Data for half-maximal voltage ($V_{50\%}$) was taken from the Boltzmann function (Fig. 2K; 11 PV cells from four mice and 10 bursting SOM cells from eight mice). Data from Fig. 2B-D & H-K were compared using a Mann-Whitney test, with alpha = 0.05. (*p<0.05, **p<0.01, ***p<0.001).

Curves of spikes per second vs. current and their quantiles were plotted using R-Project's ggplot package. The reported rheobase averages and SEMs were computed based on the current which first caused at least one spike during the stimulus per recording (Table S1). The slope averages were computed from the average least squared regression of individual curves over supports which were greater than each recording's computed rheobase. The slope SEMs were computed similarly. Both p-values were computed using the R-Project's aov built-in function. Data from Tables S1 and S2 were analyzed using t-tests (with pooled variances when the equal variance test passed) or Mann-Whitney otherwise with alpha = 0.05 (*p<0.05, **p<0.01, ***p<0.001, ****p<0.0001).

Cumulative probability distributions and KS-Test p-values (Fig. S2 B-C) were generated using the bootstrap method with 1000 iterations. sIPSC interval CDFs and p-values were generated from 17 PV and 10 SOM cells (three mice for each group) using 30 sweeps from each cell per iteration. All other sIPSC variables were generated from 12 PV and 8 SOM cells (n = 3 SOM mice, n = 5 PV mice) using 30 sweeps from each cell per iteration. sEPSC interval CDFs and p-values were generated from 14 PV and 10 SOM cells using 80 sweeps from each cell per iteration. All other sEPSC variables were generated from 11 PV and 10 SOM cells using 80 sweeps from each cell per iteration. The probability distributions were similar in SOM and PV neurons (p>0.1 for all the parameters; Table S2).

Comparison of thalamic circuit oscillations in thalamic slices

Quantification of number of active channels in VB that presented an evoked oscillatory response (Fig. 5C) and number of total evoked bursts recorded in all VB channels (Fig. 5D) was obtained from five sweeps of each recording (n = 4 slices from three PV mice, n = 5 slices from three SOM mice). All data were compared using a Mann-Whitney test, with alpha = 0.05. (*p<0.05, **p<0.01, ***p<0.001).

Analysis of cortical modulation by selective optical activation of nRT during free behavior

ECoG analysis: For induction trials, the number of oscillation cycles per recording was determined through visual observation of the mean EEG trace across all stimuli. Only oscillations evident above background noise and between

5-15 Hz were counted, and the difference between groups was analyzed using a Mann-Whitney rank sum test ($p<0.05$). Line length was extracted for the 500 ms following each 20 ms light stimulus. Raw data sampled at 24 kHz was bandpass filtered between 7-15 Hz and z-scored, then the line length was calculated as the sum of absolute differences between samples. Differences between cumulative probability distributions were quantified using the two-sample Kolmogorov-Smirnov (KS) test. CDFs were generated using data from all individual stimulus trials for each group (PVxAi32 = 2309 trials, SOMxAi32 = 2003 trials, PV-Cre = 400 trials, SOM-Cre = 1000 trials, PV+SOM- = 1400 trials).

For disruption trials, PreStim was defined as 2 s before stimulus onset, and PostStim was defined as 2 s after light stimulus, excluding the initial 200 ms of the response to avoid the large stimulus evoked transient. We calculated relative changes in root-mean-squared (RMS) power from PreStim → Stim and repeated this analysis for each condition to statistically evaluate the effect of the light on the ECoG across the different mouse groups (Fig. 7). Summary CDFs for the change in RMS power were generated using data from the ipsilateral somatosensory cortex (S1) including all valid trials for each group (PV-Cre = 40 trials, SOM-Cre = 51 trials, PV+SOM- = 47 trials).

Analysis of Somatosensory Behavior

Responses were averaged across trials per condition per mouse. Responses for evoked grooming were analyzed using a two-way mixed model ANOVA with genotype (PV-Cre x Ai32 or SOM-Cre x Ai32) as one factor and treatment (sham1, light, sham2, light alone – no tape) as the repeated measures factor. Posthoc multiple comparison tests (Sidak's) were used to determine whether treatment conditions were significantly different from Sham1 within groups. Alpha was set to 0.05 and adjusted for 6 comparisons ($*p<0.05$).